Mercurian sphalerite from Akoluk deposit (Ordu, NE Turkey): Hg as a cathodoluminescence activator

Article *in* Mineralogical Magazine · April 2009

DOI: 10.1180/minmag.2009.073.2.257

Emin Çiftçi
Istanbul Technical University

Mineralogical Magazine, April 2009, Vol. 73(2), pp. 165–175

Mercurian sphalerite from Akoluk deposit (Ordu, NE Turkey): Hg as a cathodoluminescence activator

E. Çiftçi*

Nigde University, Department of Geological Engineering, 51245 Nigde, Turkey

[*Received 14 March 2008; Accepted 16 April 2009*]

ABSTRACT

A recent investigation of sphalerite from Akoluk deposit, Ordu, NE Turkey, revealed the possible presence of a new activator element in the sphalerite structure. The sample was studied under a reflected light microscope coupled with a cold-stage cathodoluminescence (CL) system which revealed a unique banding in the sphalerite. The same sample was subsequently examined using the back-scattered electron and luminescence modes in an electron microscope, the results of which were later confirmed by electron probe microanalyses (EPMA) in terms of chemical composition. Detailed evaluation of the EPMA data indicated the presence of a new CL activator element in the sphalerite structure. The data also indicate that Hg^{2+} in the sphalerite crystal structure substitutes for Zn in a simple manner and for Cd and Cu in a coupled manner. Spectral analysis indicated a bright yellow and orange-red blend (more like brown) CL colour with λ_{max} centred at 580 nm, probably due to Cd and Mn ions, and relatively broad emission bands ranging from 525 to 690 nm with λ_{max} centred at 580 and 700, due probably to Cu, Cd and Hg. This study reports that Hg in the sphalerite crystal lattice behaves as an activator and/or co-activator element resulting in emissions of CL colours that range from yellow with purple shades to shades of brown, based on their varying contents.

Keywords: sphalerite, mercury, activator, Akoluk, cathodoluminescence, Turkey.

Introduction

Cathodoluminescence is the emission of photons with wavelengths ranging from ultraviolet to infrared caused by excitation from an electron gun. The cathodoluminescence of minerals can be categorized as either intrinsic or extrinsic. The intrinsic CL centre is native to the host materials and it involves band-to-band recombination of electron and hole pairs. Intrinsic CL emission may also be associated with lattice defects (e.g. anion vacancies) within those minerals. This type of CL is also said to be a 'defect' CL centre. Extrinsic CL emission includes radiation-induced defects, electron defects on broken bonds (Götze, 2002), and the trace elements, which themselves constitute defects in the crystal structure since they distort the shape of the structure and modify the electron distributions. Although intrinsic luminescence may be a significant phenomenon, the most commonly identified CL centres in the minerals are extrinsic ones that can be attributed to the presence of trace amounts of impurities, transition metal and rare earth ions. Commonly, natural minerals and synthetic materials are not pure. Consequently, some of the minerals may contain optically active dopant ions, which can be categorized in three groups that strongly influence and often dominate the net CL of a particular mineral: (1) activators, (2) sensitizers, and (3) quenchers. While activators produce CL by releasing the absorbed energy as photons – the most common activators present in natural minerals are transition metal ions (Cr^{3+}, Mn^{2+}, Fe^{3+}) and rare earth elements ($REE^{2+/3+}$) – the sensitizers absorb the energy and subsequently

---

* E-mail: eciftci@nigde.edu.tr

DOI: 10.1180/minmag.2009.073.2.165

transfer that energy to activators. On the other hand, the quenchers trap part or all of the absorbed energy resulting in non-radiative decaying of the energy eliminating the CL in minerals (i.e. Fe^{2+} is a well known quencher). As a result, many sulphide, silicate and carbonate minerals with more than minor ferrous iron contents are non-luminescent.

In geological applications employing the CL microscope (CLM), the CL emissions with wavelengths only in the visible range are of primary interest. The CL is a near-surface characterization technique. The penetration depth of electrons, depending on the energy of the electrons, is in the range of 2 to 8 μm. Unless the grains are zoned, the information obtained is assumed to be representative of the whole particle/grain or crystal. Trace element-activated CL may often involve activator and sensitizer elements in concentrations from 1000s to <10 ppm. Hence techniques such as EPMA may not be sufficiently sensitive to enable detection of all activators, sensitizers and quenchers, leading to only partial understanding of the CL. Methods such as secondary ion mass spectrometry (SIMS), proton induced X-ray emission (PIXE) and laser ablation-inductively coupled plasma mass spectrometry (LA-ICPMS) are required for more complete characterization of the trace element chemistry. These methods however use relatively large 'spot' sizes and may lack the spatial resolution in samples that are small and/or chemically zoned at fine scales.

Cathodoluminescence is used widely in the materials sciences (Karakus, 2006) and in various branches of the geological sciences including ore genesis, sedimentology, petrology and structural geology (Marshall, 1988; Kuhlemann *et al.*, 2001; Wallace *et al.*, 1994; Thomas *et al.*, 1991; Stirling *et al.*, 1999; Ramseyer *et al.*, 1992; Laubach *et al.*, 2004; Onasch and Davis, 1988).

Sphalerite occurs in ore mineral parageneses as the major component of a large variety of Pb-Zn deposits, such as vein-type, skarn, and massive sulphide deposits. The mineral chemistry of sphalerite has commonly been used to decipher the principal conditions governing the ore deposition since its composition is a complex function of pressure, temperature and sulphur activity. The CL characteristics of sphalerite ore from various ore deposits worldwide may also be used to distinguish between sphalerite generations, crystal-growth mechanisms and changes in conditions during ore-mineral deposition, as CL enhances internal structures that are imperceptible to other microscopic techniques (Karakus *et al.*, 2008; Kuhlemann *et al.*, 2001; Kuhlemann and Zeeh, 1995).

CL characteristics of natural sphalerites

Sphalerite is one of the few sulphide minerals that can be studied under the CLM, because it is one of the few in which Fe does not quench CL emissions up to ~1.5 wt.%. The sphalerite crystal structure consists of a face-centred cube in which the face centres and corners are occupied by Zn atoms that are tetrahedrally coordinated with four S atoms, and *vice versa*, the S atoms are coordinated in a tetrahedral manner in that the each S atom is located at the centre of a regular tetrahedron of Zn atoms. In the sphalerite structure, substitution for Zn occurs in two ways: either stable divalent cations of certain elements including Fe, Cd, Mn, Hg, Cu, Co, Ni, Ge, Ti, W, Ga, Pb, Sn and In substitute for Zn in tetrahedral sites to varying extents or coupled substitution of any of the above for two Zn ions. Coupled substitution enables monovalent Cu and Ag ions or trivalent Fe ions to enter the sphalerite structure as well. The cation distribution within each CL zone has been assumed to be completely random (Spalek *et al.*, 1986) and/or as bands produced by a segregation of substituents (Johan, 1988; Pattrick *et al.*, 1993). It has also been reported that the Co^{2+}- and Ni^{2+}-doped ZnS structures are luminescent (Kazanskii *et al.*, 1969). However, no natural occurrence of either has been reported to date.

The sphalerite structure is an important artificial phosphor (Leverenz, 1968; Marfunin, 1979). Other studies of natural sphalerites include those by Kyle and Price (1985) and Zeeh and Kuhlemann (1996). Pure synthetic sphalerite shows an intrinsic blue luminescence, caused by the formation of a wurtzite-sphalerite twin and of other structural defects (Gumlich and Reihl, 1971). By contrast, most natural sphalerites do not luminesce due to the presence of the common quencher, Fe^{2+}. However, a large variety of cathodoluminescence colours associated with sphalerite and wurtzite (the other dimorph of zinc sulphide) has been observed, mainly due to trace element CL activators.

The presence of Hg in the sphalerite structure as a substitute for Zn has long been known. The term 'mercurian sphalerite' has been used to describe such sphalerite ores. The best known examples are the Eskay Creek deposit (Canada), where mercury may constitute as much as 15 wt.% of the sphalerite structure (Grammatikopoulos *et al.*, 2006), the Broken Hill deposit (Australia) (Ryall, 1979), the Levigliani and Ripa deposits (Italy) (Dini *et al.*, 2001), the East Alpine deposits (Austria–Slovenia) (Kuhlemann and Zeeh, 1995), and natural sphalerites from various deposits (Benedetto *et al.*, 2005). Table 1 lists the CL activators and their colours from sphalerites of various deposits. The sphalerite crystal from the Akoluk deposit (Turkey) studied here contains as much as ~5 wt.% **(author: of Hg?)** (Table 2). Study of the CL in sphalerite crystals in the present is due mainly to Hg and to a lesser extent to Cd and Cu. Based on the EPMA data, the presence of Hg in the sphalerite structure is evaluated, and the variation in CL colour with increasing Hg content is interpreted.

Materials and analytical methods

Sample description

The sample studied was taken from a deposit (formally referred to as Akoluk, locally known as the Ohtamiş deposit) located in the northwestern segment of the eastern Black Sea Region (Turkey), ~20–25 km from the Black Sea coast (Fig. 1). The region is considered to be a palaeoarc environment and it hosts a large variety of ore deposits including Kuroko-type, massive sulphide, epi-mesothermal vein-type, and skarn deposits (Ciftci, 2000). The study area comprises volcanic and sedimentary rocks ranging from Upper Cretaceous to Eocene in age. The oldest rocks near the deposit are the felsic volcanic rocks, the so-called pyritized dacite lava, pyroclastics and tuffs which host the mineralization of interest. The ore mineralization was controlled by pre-existing fault systems striking NE–SW and thus can be

TABLE 1. CL-activator elements and associated CL colours reported from various ore deposits.

CL-activator	CL-colour	Locality
Ag^+	Blue, light blue	East Alpine, Austria–Slovenia[1, 2, 3]
Cu-Pb-Ag-Cd	Orange-red	East Alpine, Austria–Slovenia[1]
Tl, As, Ge, Fe	Brown	East Alpine, Austria–Slovenia[1]
Cu-Pb-Cd	Red-Orange-red	East Alpine, Austria–Slovenia[1, 2]
Cd^{2+}-Ag^+	Orange-red	East Alpine, Austria–Slovenia[1, 2]
Cd^{2+}	Blue	Not specified, Europe/Algeria[2]
Mn^{2+}	Yellow	Not specified, Europe/Algeria[2]
Ag^+-Ga^{3+}	Orange	Horn Silver, USA[3]
Pb^{2+}-Cu^+	Bright green	ZC#2 mine, USA[3]
Ga^{3+}-Ag^+	Shades of violet	Tsumeb, Namibia[3]
Cu-Ag	Orange-red	East Alpine, Austria–Slovenia[1]
Cu-Pb	Orange-red	East Alpine, Austria–Slovenia[1]
Cu-Ga/In	Orange-red	Not specified[4]
Cu-Ag-In-Ga-Tl	Orange-red	Not specified[5]
Ge-Cu	Green	Kipushi, Zaïre[6]
Ga-Cu	Red	Kipushi, Zaïre[6]
Mn^{2+}	Orange-yellow	Orpierre, France[6, 3]
Cd^{2+}	Yellow	Tirol, Austria[6]
Cu-Tl^{3+}	Orange-red	Not specified[7]
Cd^{2+}	Greenish yellow-reddish orange	Hockley salt-dome, USA[8]
Ag^+-Cd^{2+}	Reddish orange	Hockley salt-dome, USA[8]
Cd^{2+}-Ag^+	Greenish-yellow	Hockley salt-dome, USA[8]
Cu	Green	East Alpine, Austria–Slovenia[1, 9]
Co^{2+}	Green	Dill Syncline, Germany*[10]
Hg-Cd-Cu	Yellow-dark yellow-shades of brown	Akoluk Deposit, Turkey**

[1] Kuhlemann and Zeeh (1995); [2] Haberlandt and Schroll (1950); [3] Karakus *et al.* (2008); [4] Platonov and Tarashchan (1967); [5] Tarashchan and Platonov (1968); [6] Goni and Rémond (1969); [7] Marfunin (1979); [8] Kyle and Price (1985); [9] Gumlich and Riehl (1971); [10] Rager *et al.* (1996)

* visible colour; ** reported in the current study.

TABLE 2. Chemical compositions as determined through EPMA analyses of selected micro-areas within the sphalerite crystal as shown in Figure 2 (values are in wt. %; values as ppm in parenthesis are detection limits for trace constituents).

Element	1	2	3	4	5	6	7	8	9
As (>150)	0.020	0.029	0.029	0.006	0.021	0.003	0.020	0.003	0.005
Zn	66.808	63.137	65.951	67.264	67.285	66.085	60.498	66.085	63.144
S	31.905	31.500	32.039	32.134	32.084	31.932	30.800	31.932	31.201
Pb (>200)	0.116	0.092	0.090	0.134	0.110	0.062	0.129	0.062	0.045
Hg (>250)	0.928	3.975	1.776	0.650	0.741	1.437	4.815	1.437	3.947
Fe (>100)	0.027	0.024	0.040	0.048	0.059	0.020	0.012	0.020	0.027
Mn (>80)	n.d.	n.d.	n.d.	n.d.	0.013	n.d.	n.d.	n.d.	n.d.
Ti (>150)	n.d.	n.d.	0.018	n.d.	n.d.	0.018	0.015	0.0180	n.d.
Ag (>200)	n.d.	0.112	n.d.	n.d.	0.001	0.025	0.109	0.025	0.025
Cd (>200)	0.200	0.754	0.434	0.279	0.618	0.533	1.649	0.533	1.270
Cu (>80)	n.d.	0.325	0.059	n.d.	n.d.	0.002	0.592	0.002	0.075
Ge (>250)	n.d.	0.088	n.d.	n.d.	n.d.	n.d.	n.d.	n.d.	n.d.
Total	100.004	100.036	100.440	100.515	100.930	100.120	98.640	100.120	99.770
Element	10	11	12	13	14	15	16	17	18
As	0.007	n.d.	0.014	0.050	0.011	0.014	0.001	n.d.	0.006
Zn	66.675	66.735	64.264	63.078	61.136	63.515	64.619	67.933	67.264
S	32.125	32.255	31.600	30.873	30.992	30.987	31.447	32.461	32.134
Pb	0.087	0.098	0.221	0.079	0.223	0.141	0.149	0.101	0.134
Hg	1.475	1.429	2.787	4.385	4.784	3.544	3.485	0.001	0.650
Fe	0.029	0.001	0.048	0.016	0.054	0.054	0.011	0.040	0.048
Mn	0.020	0.013	0.022	n.d.	n.d.	0.023	n.d.	0.024	n.d.
Ti	0.018	0.002	0.002	n.d.	0.015	n.d.	n.d.	n.d.	n.d.
Ag	n.d.	n.d.	0.017	0.015	0.04	0.069	0.021	n.d.	n.d.
Cd	0.411	0.348	0.710	1.260	1.883	1.932	0.858	0.377	0.279
Cu	n.d.	n.d.	n.d.	0.038	0.251	0.385	0.040	n.d.	n.d.
Ge	n.d.	n.d.	n.d.	n.d.	n.d.	n.d.	n.d.	n.d.	n.d.
Total	100.847	100.880	99.690	99.794	99.390	100.664	100.630	100.940	100.515

n.d.: not detected

considered as a structurally controlled epi-mesothermal vein-type deposit. The major ore minerals are stibnite, zinkenite, sphalerite, pyrite, galena and native gold with associated quartz, baryte and a number of clay minerals that account for gangue phases. Mining of this mineralization is currently under development. Other characteristics (such as fluid inclusions, stable isotope and ore-mineral paragenesis), confirm the interpretation of this deposit as an epi-mesothermal mineralization (Ciftci, 2000).

Analytical methods

The samples examined were collected from an exploration trench which is considered to be representative of the major ore types present in the deposit. Polished sections were prepared for both reflected light microscopy coupled with CL (University of Missouri-Rolla, Missouri, USA) and electron probe microanalysis (Indiana University, Bloomington, Indiana, USA) by following standard preparation and polishing steps (Picot and Johan, 1982).

A CITL (Cambridge Image Technology Ltd.), Cold Cathode Luminescence, Model 8200 Mk3 mounted on a Nikon Labophot-2-Pol microscope with Optronics 3CCD video imaging system, Model DEI 750 was used in this study. The system was operated at an electron energy of 8–15 kV, probe current of 500–800 mA and an operating vacuum of 100 to 1000 mbar. The CL spectra were acquired using an Oceans Optics High Resolution Fiber Optic Spectrometer with 1.5 nm optical resolution for the wavelength range of 350 and 850 nm.

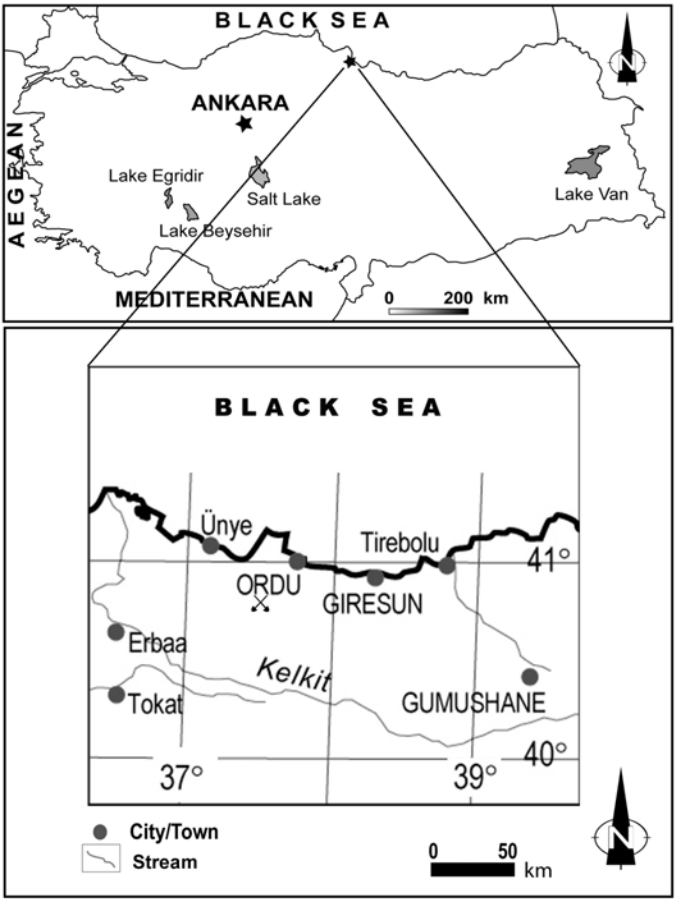

FIG. 1. Map of the study area showing where mercurian sphalerite is part of the primary sulphide mineralization.

The composition of the sphalerite was determined by wavelength dispersive X-ray analysis using a Cameca SX50 electron microprobe. An accelerating voltage of 15 kV was used. The probe current and counting time for the major elements were 20 nA and 20 s, respectively. Trace elements were analysed at a probe current of 100 nA and a counting time of 30 s with a 1–10 µm beam diameter, depending on the width of the bands. The accuracy of the EPMA analyses was monitored using reference material of similar composition. The analytical results and detection limits for each of the trace constituents are listed in Table 2. The sphalerite analyses are from points within homogenous areas in each band. A correlation analysis was also carried out to determine quantitative and correlative behavior of major and trace elements.

Results

Figure 2 shows corresponding images of the same area acquired using a reflected light microscope (RLM), the CLM and EPMA-back-scattered electron imaging (BSEI) techniques. Sphalerite crystals from the study area typically cathodoluminesce in yellow. This is attributed to their Cd^{2+} content because, in general, Cd^{2+} as a CL centre and emits a yellow colour (Goni and Rémond, 1969; Kyle and Price, 1985; Karakus *et al.*, 2008). In most sphalerites from the study area, Cd was always present at wt.% levels. Manganese, on the other hand, when present in trace amount, acts as a CL centre and emits an orange-yellow colour (Karakus *et al.*, 2008; Goni and Remond, 1969; Kuhlemann and Zeeh, 1995). The Mn in the sphalerite sample studied was generally below the

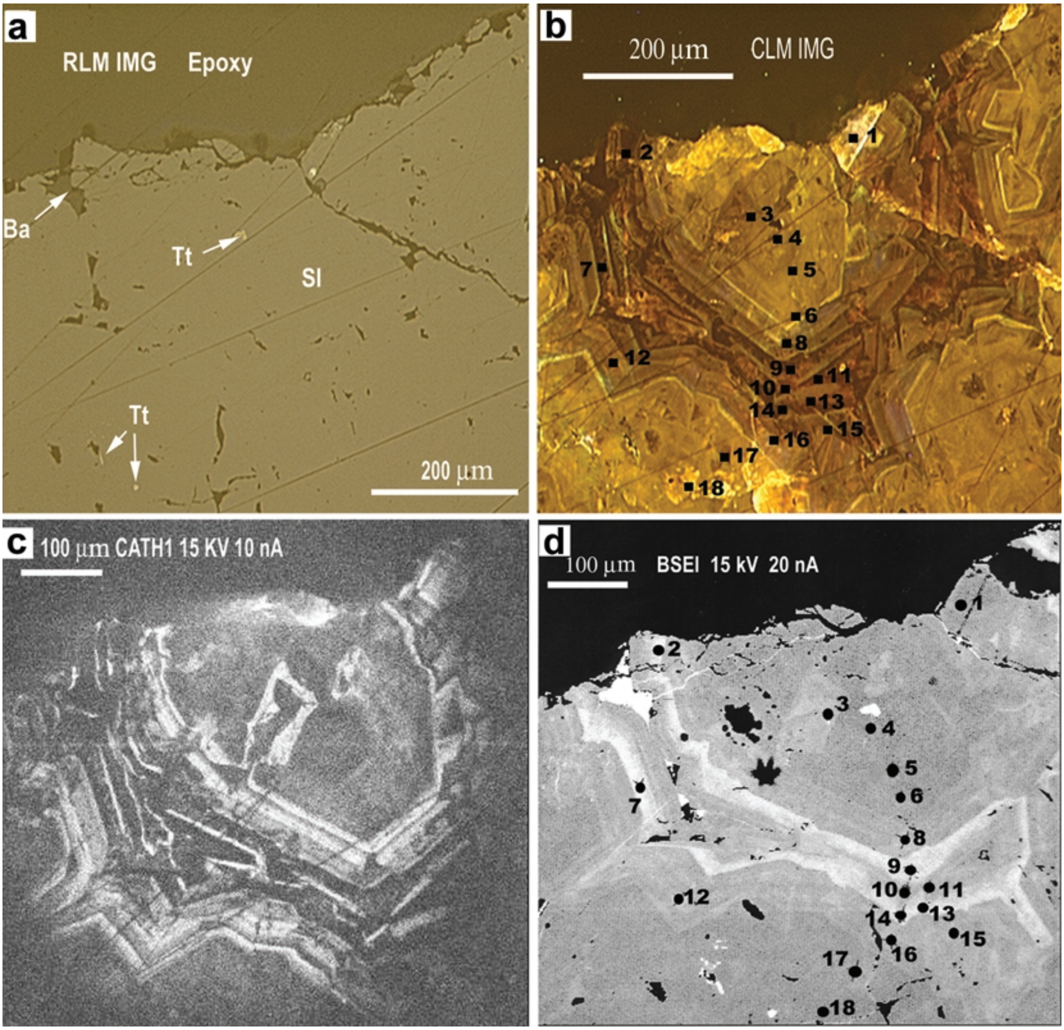

FIG. 2. (*a*) RLM image of the sphalerite (Sl) in which baryte (Ba) and tetrahedrite (Tt) encapsulations occur; (*b*) CLM image of the same area. Sl is mainly yellow and brown-yellow rhythmic bands occur as a result of changes in the Sl chemistry; (*c*) electron microscope cathode mode image which matches exactly the CLM image; and (*d*) BSEI of the same crystal. The bands are due to changes in chemical composition. The lighter colour indicates an increase in the heavy element contents (see the EPMA data in Table 1).

detection limit (<~80 ppm). Because of its limited presence or absence, as shown by some of the EPMA point analyses, an earlier report on the chemistry of major sulphide ores of the deposit (Ciftci, 2000), and spectral analysis of the observed spectra, compared with known spectra, the yellow CL colour in the present sample was attributed to Cd rather than to Mn. Any Fe present is always at levels less than the critical level, ~0.08−0.1 wt.% (Karakus *et al.*, 2008), above which it acts as strong quencher and no visible, room-temperature CL would have been observed.

In the sphalerite crystal studied here, the typical yellow colour changes outwards to yellow with a purple tint, dark yellow, light brown, and then dark brown due to an increase in the Hg, Cd and Cu contents (Fig. 2*b*). The EPMA measurements are taken from within the zones identified in the CL (Fig. 2*b*) and BSE (Fig. 2*d*) images. The results are given in Table 2.

Figure 3*a*,*b* shows the variations of common elements occurring in the sphalerite structure from micro-points 1 to 18. Corresponding colour variations along the points also are given in Figure 3*b*,*d*. Figures 4*a* and 4*b* are CL spectra for a sketched map of the major zones of sphalerite.

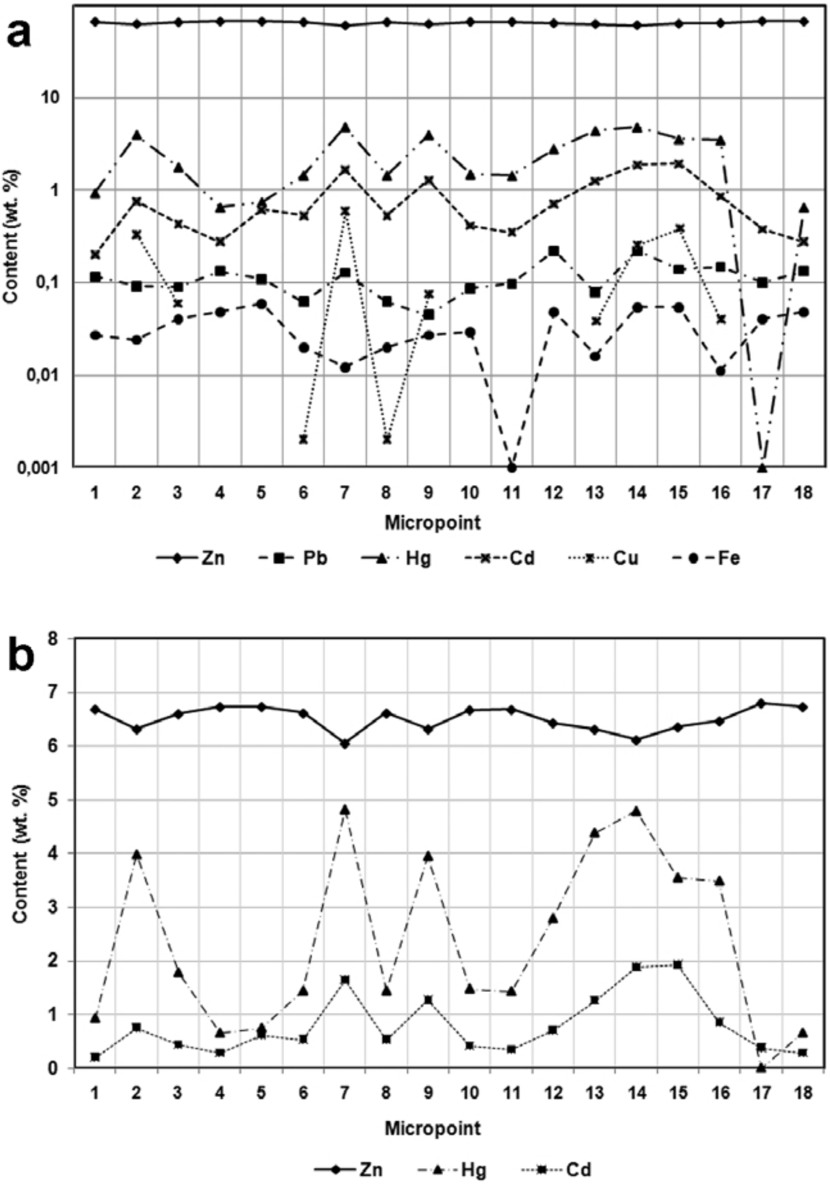

FIG. 3. (*a*) Element distribution from micropoints 1 to 18 in sphalerite crystals analysed for major and trace constituents (>0.01% level on the vertical axes represents the detection limit for the elements of interest); (*b*) Zn, Hg and Cd variations along the same line indicating coupled replacement of Hg and Cd for Zn in tetrahedral sites, which resulted in the colour change from yellow to dark brown (A – yellow, B – brown, C – dark yellow, D – dark brown, E – dark yellow with purple tint, F – light brown, G – dark yellow with purple tint, H – light brown-dark brown, K – dark yellow with purple tint-yellow) (all of the information in the plot lies above detection limit for the elements shown).

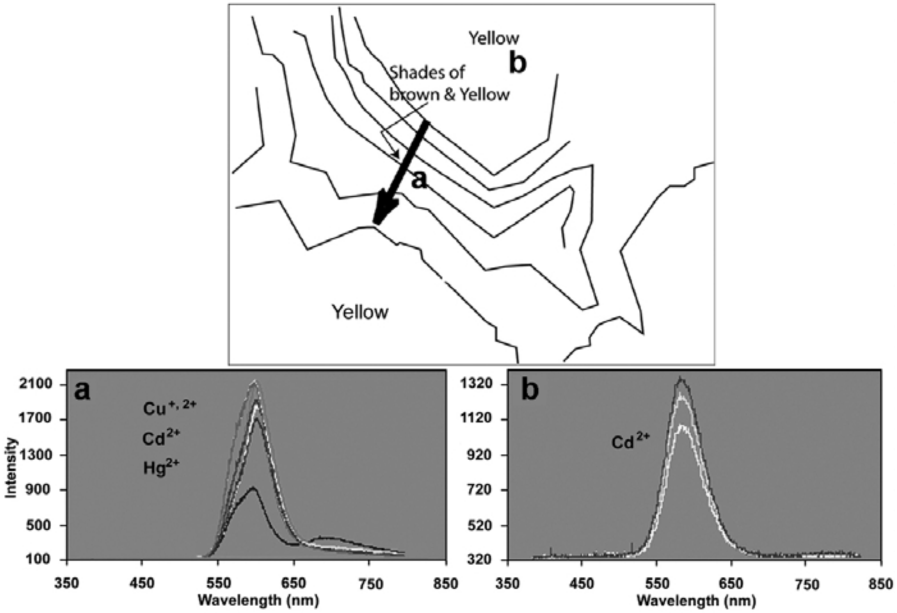

FIG. 4. (*a*) CL spectra obtained from the sphalerite crystal for the area showing zonation and (*b*) from an area of homogeneous yellow colour.

Correlation analysis was carried out to determine and evaluate trace elements present and the relationship between them. As can be seen in Table 3, based on the Pearson correlation coefficients, strong positive correlations (R >+0.5) occur between Hg-Cd, Mn-Zn, Hg-Ag, Cd-Ag, Hg-Cu, Cd-Cu, and Cu-Ag. Strong negative correlations (R <−0.5) exist between Zn-Hg, Zn-Cd, Zn-Ag, Zn-Cu, Hg-Mn, Cd-Mn, and Mn-Ti. Strong positive and negative correlations can be seen in Figures 3*a* and 3*b*. Figure 3*a* shows variations of the common trace elements in the sphalerite structure along the EPMA analyses traversing the CL zones and Figure 3*b* shows visible CL colour variation embedded within the EPMA data for selected elements.

Discussion

Trace element partitioning into the sphalerite structure is controlled essentially by Goldschmidt's rules and the availability of such

TABLE 3. Correlation matrix between cations detected in the sphalerite structure. Cells show the Pearson correlation coefficient.

	Zn	Hg	Cd	Pb	Fe	Mn	Ti	Ag	Cu
Hg	−0.971								
Cd	−0.941	0.903							
Pb	−0.428	0.411	0.408						
Fe	0.076	−0.153	0.085	0.391					
Mn	0.548	−0.609	−0.518	0.215	0.311				
Ti	−0.373	0.268	0.288	0.013	−0.011	−0.590			
Ag	−0.834	0.740	0.764	0.192	−0.284	−0.452	0.429		
Cu	−0.812	0.704	0.775	0.215	−0.186	−0.437	0.471	0.947	
As	−0.210	0.130	0.152	0.150	0.470	−0.183	0.445	0.205	0.351

trace elements in the environment. The ore-mineral paragenesis of the Akoluk deposit suggests that the primary sulphide ore minerals were deposited under reducing conditions and that the CL activators, Hg, Cd, Mn and Cu were not abundant enough to crystallize as distinct minerals (since Mn was below the detection limit and its characteristic CL colours were not observed, it is no longer considered here). During the crystal growth of sphalerite, local enrichments of any or all three elements should have occurred resulting in the replacement of Zn^{2+} in the tetrahedral sites in a coupled manner (any pair of divalent trace metals, e.g. Hg^{2+} and Cd^{2+} for two Zn^{2+}) and/or simple manner (any of divalent trace metals for Zn^{2+}). The scarcity of similar luminescent banding in sphalerites associated with Hg, Cd, and Cu indicates that in the majority of the cases, the system either lacked those trace elements, or that these elements, together or in varying proportions, entered into other coeval sulphide minerals structures, such as tetrahedrite, stibnite, and galena. However, the EPMA data from Ciftci (2000) showed that Hg and Cd, in particular, occur strictly with sphalerite, thus ruling out the latter situation. In addition, activation was prevented by other features of the mineral chemistry that were inaccessible in the present study.

Cadmium is a known CL activator in sphalerite structures. It can produce CL alone or coupled with Ag (Karakus *et al.*, 2008; Kyle and Price, 1985; McKeag and Steward, 1957). Earlier reports indicate that it alone may account for bright yellow, greenish yellow-reddish orange and blue, and with Ag, for orange red, reddish orange and greenish yellow. For such diverse CL emissions, in addition to other coupling elements including Ag, defects influencing the electron transitions within the Cd ions could be involved. Copper is also a known CL activator in sphalerite structures. It can produce blue and/or green CL colour alone or coupled with Pb causing orange-red CL colour emission (Table 1). The presence of Hg in sphalerite structures in trace quantities has also long been known. There are some ore deposits in which Hg is enriched in sphalerite at wt.% levels (Ryall, 1979; Rytuba, 2003; Grammatikopoulos *et al.*, 2006). However, there are no reports of the CL characteristics of such mercurian sphalerites due either to lack of investigation or to the non-luminescencing behaviour of those sphalerites, perhaps because of the presence of CL quenchers. Sphalerite samples from Eskay Creek and Broken Hill were also investigated for CL behaviour to test Hg-induced CL behavior but neither of these samples cathodoluminesced at a detectable level by a low-light CCD camera and spectrometer. Knowing that the Hg content of those sphalerites was reportedly >>10 wt.%. The fact that it does not cathodoluminesce could be attributed to the abundance of Hg. However, impurity-free sphalerites doped with varying amounts of Hg should be investigated to determine the critical level of Hg abundance beyond which it acts as a quencher.

The Cd, Cu and Hg replacing Zn may act as CL-producing centres and result in emissions perceived by the eye as shades of brown based on the extent of such replacement. As is the case for many trace element activators in many other CL-luminescent minerals, excessive amounts of such trace elements can behave as CL quenchers. The darkening of some areas in Fig. 2*b* is interpreted to indicate that in amounts >~7 wt.% combined, those elements tend to behave as CL quenchers. Due to the lack of data from synthetically crystallized sphalerites containing Hg under controlled conditions, the CL behavior of sphalerites above this amount is not known with certainty. Those sphalerites would be expected to be non-luminescent as is the case for the Eskay Creek sphalerite.

Although there have been reports on the individual effects of Cd on the CL behaviour of sphalerite (Table 1), there are no data on the effect of Hg alone on the CL characteristics of sphalerite. In this particular crystal, tints of purple in yellow areas could be attributed to the presence of Ag since it may cause emission of blue as reported earlier (Kuhlemann and Zeeh, 1995; Haberlandt and Schroll, 1950; Karakus *et al.*, 2008). The Cd alone or coupled with Ag did not account for the brownish colour. Thus, it is interpreted here that the brown colours are produced mainly by the presence of Hg.

There have been reports on the individual and combined effect of Cu with Pb on the CL behavior of sphalerite (Table 1). However, there is no study on its effect with Hg. Thus it is assumed here that bluish tints could be generated by Ag since it was detected chemically in corresponding zones.

Table 3 lists correlation matrices for all of the elements detected in the sphalerite structure. In addition to the strong negative correlations of Hg-Cd-Cu with Zn, the behaviours of Ag and Pb may also be significant since they also show positive correlations with Hg, Cd and Cu. Although Ag and Pb are reported to be CL-impurity centres in the sphalerite structure as listed in Table 1, due to their low quantities and scattered presence, they are not expected to produce such zonal CL colours in this particular case.

Acknowledgements

This project was funded by the Scientific and Technological Research Council of Turkey (TUBITAK) through the financial support program (program I.D. 2219) for post-doctoral studies carried out abroad. The author thanks Dr Richard D. Hagni (Missouri University of Science and Technology) and Dr Tassos A. Grammatikopoulos (MacGill University, Canada) for providing sphalerite samples and Dr Anthony N. Mariano for his contributions and constructive criticisms which significantly improved the manuscript and Dr Musa Karakus (CCI Inc.) for his kind help with the CLM study. Dr Edward M. Ripley and Dr Chusi Li (Indiana University, Bloomington) are also thanked for their help with microprobe analyses carried out at their facilities.

References

Benedetto, F.D., Bernardini, G.P., Costagliola, P., Plant, D. and Vaughan, D.J. (2005) Compositional zoning in sphalerite crystals. *American Mineralogist*, **90**, 1384–1392.

Ciftci, E. (2000) *Mineralogy, paragenetic sequence, geochemistry and genesis of the gold and silver bearing Upper Cretaceous mineral deposits, northeastern Turkey*. PhD Dissertation (unpublished), University of Missouri-Rolla, 251 pp, Missouri, USA.

Dini, A., Benvenuti, M., Costagliola, P. and Lattanzi, P. (2001) Mercury deposits in metamorphic settings: the example of Levigliani and Ripa mines, Apuane Alps (Tuscany, Italy). *Ore Geology Reviews*, **18**, 149–167.

Goni, J. and Rémond, G. (1969) Localization and distribution of impurities in blende by cathodoluminescence. *Mineralogical Magazine*, **37**, 153–155.

Götze, J. (2002) Potential of cathodoluminescence (CL) microscopy and spectroscopy for the analysis of minerals and materials. *Analytical and Bioanalytical Chemistry*, **374(4)**, 703–708.

Grammatikopoulos, T.A., Valeyev, O. and Roth, T. (2006) Compositional variation in Hg-bearing sphalerite from the polymetallic Eskay Creek deposit, British Columbia, Canada. *Chemie der Erde*, **66(4)**, 307–314.

Gumlich, H.E. and Reihl, N. (1971) Phosphore der ZnS-Gruppe (II-IV-Verbindungen). Pp. 35–109 in: *Einführung in die Lumineszenz* (N. Reihl, editor). Karl Thiemig, München, Germany.

Haberlandt, H. and Schroll, E. *(*1950) Lumineszierende Anwachszonen in der Zinkblende yon Bleiberg-Kreuth (Karnten, Österreich). *Experientia*, **V1**, 91–92.

Johan, Z. (1988) Indium and germanium in the structure of sphalerite: an example of coupled substitution with copper. *Mineralogy and Petrology*, **39**, 211–229.

Karakus, M. (2006) Cathodoluminescence microscopy and spectroscopy characterization of refractory and advanced structural ceramics. *UNITECR '05 - Proceedings of the Unified International Technical Conference on Refractories: 9th Biennial Worldwide Congress on Refractories*, pp. 330–334.

Karakus, M., Hagni, R.D., Koenig, A. and Çiftçi, E. (2008) Cathodoluminescence, Laser Ablasion Inductively Coupled Plasma Mass Spectrometry, Electron Probe Microanalysis and Electron Paramagnetic Resonance Analyses of Natural Sphalerite. *ICAM 2008 Proceedings*, pp. 112–124, Brisbane, Australia.

Kazanskii, S.A., Ryskin, A.I. and Khil'ko, G.I. (1969) Effect of bonding character on the spectra of Co^{2+} and Ni^{2+} ions in ZnS crystals containing stacking faults. *Soviet Physics – Solid State*, **10**, 1899–1902.

Kuhlemann, J. and Zeeh, S. (1995) Sphalerite stratigraphy and trace element composition of East Alpine Pb-Zn deposits (Drau Range, Austria-Slovenia). *Economic Geology*, **90**, 2073–2080.

Kuhlemann, J., Vennemann, T., Herlec, U., Zeeh, S., and Bechstadt, T. (2001) Variations of sulfur isotopes, trace element compositions, and cathodoluminescence of Mississippi Valley-type Pb-Zn ores from the Drau Range, eastern Alps (Slovenia–Austria): implications for ore deposition on a regional versus microscale. *Economic Geology*, **96**, 1931–1941.

Kyle, J. R. and Price, P. E. (1985) Mineralogical investigation of sulfide concentrations in the Hockley salt dome cap rock, Texas. Pp. 1065–1082 in: *Applied Mineralogy* (W.C. Park *et al*., editors). Metallurgical Society of the AIME.

Laubach, S.E., Reed, R.M., Olson, J.E., Lander, R.H. and Bonnell, L.M. (2004) Co-evolution of crack-seal texture and fracture porosity in sedimentary rocks: cathodoluminescence observations of regional fractures. *Journal of Structural Geology*, **26**, 967–982.

Leverenz, H.W. (1968) *An Introduction to Luminescence of Solids*. Dover Publications, New York.

Marfunin, A.S. (1979) *Spectroscopy Luminescence and*

Radiation Centers in Minerals. Springer-Verlag, Berlin, 352 pp.

Marshall, J.D. (1988) *Cathodoluminescence of Geological Materials*. Unwin Hyman, London, 146 pp.

McKeag, A.H. and Steward, E.G. (1957) Effect of crystal disorder on the electroluminescence of zinc sulfide phosphors. *Journal of the Electrochemical Society*, **104**, 41–45.

Onasch, C.M. and Davis, T.L. (1988) Strain determination using cathodoluminescence of calcite overgrowths. *Journal of Structural Geology*, **10**, 301–303.

Pattrick, R.A.D., Dorling, M. and Poyla, D.A. (1993) TEM study of indium and copper-bearing growth-banded sphalerite. *The Canadian Mineralogist*, **31**, 105–117.

Picot, P. and Johan, Z. (1982) *Atlas of Ore Minerals*. Elsevier, Amsterdam, 458 p.

Platanov, A.N. and Tarashchan, A.N. (1967) Red photoluminescence in natural sphalerites. *Doklady Akademii Nauk*, **177**, 415–417.

Rager, H., Amthauer, G., Bernroider, M. and Schurmann, K. (1996) Colour, crystal chemistry, and mineral association of a green sphalerite from Steinperf, Dill Syncline, FRG. European Journal of Mineralogy, **8**, 1191–1198.

Ramseyer, K., Aldahan, A.A., Collini, B. and Landström, O. (1992) Petrological modifications in granitic rocks from the Siljan impact structure: evidence from cathodoluminescence. *Tectonophysics*, **216**, 195–204.

Ryall, W.R. (1979) Mercury in Broken Hill (NSW, Australia) lead-zinc-silver lodes. *Journal of Geochemical Exploration*, **11**,175–194.

Rytuba, J.J. (2003) Mercury from mineral deposits and potential environmental impact. *Environmental Geology*, **43**, 326–338.

Spalek, J., Lewicki, A., Tarnawski, Z., Furdyna, J.K., Galazka, R.R. and Obuszko, Z. (1986) Magnetic susceptibility of semimagnetic semiconductors: the high-temperature regime and the role of superexchange. *Physical Reviews (B)*, **33**, 3407–3418.

Stirling, D., Duncan, A.M., Guest, J.E. and Finch, A.A. (1999) Petrogenesis of plagioclase phenocrysts of Mount Etna, Sicily, with particular reference to the 1983 eruption: Contribution from cathodoluminescence petrography. *Mineralogical Magazine*, **63**, 189–198.

Tarashchan, A.N. and Platonov, A.N. (1968) Luminescence spectra of sphalerites. *Geokhimiya*, **2**, 173–179.

Thomas, C.A., Hagni, R.D. and Berendsen, P. (1991) Ore microscopy of the Paoli silver-copper deposit, Oklahoma. *Ore Geology Reviews*, **6**, 229–244.

Wallace, M.W., Both, R.A., Ruano, S.M., Hach-Ali, P.F. and Lees, T. (1994) Zebra textures from carbonate-hosted sulfide deposits: sheet cavity networks produced by fracture and solution enlargement. *Economic Geology*, **89**, 1183–1191.

Zeeh, S. and Kuhlemann, J. (1996) Luminescence and geochemical composition of sphalerite: an example from the Alpine lead-zinc deposits (Austria/Slovenia). *International Conference on Cathodoluminescence and Related Techniques in Geosciences and Geomaterials: Nancy, France, Abstracts*, pp. 171–172.